Available online at www.sciencedirect.com
SCIENCE DIRECT
International Journal of Heat and Mass Transfer 49 (2006) 3929–3941
International Journal of HEAT and MASS TRANSFER
www.elsevier.com/locate/ijhmt

Conjugate heat transfer study of backward-facing step flow – A benchmark problem

P. Rajesh Kanna, Manab Kumar Das *

Department of Mechanical Engineering, Indian Institute of Technology Guwahati, North Guwahati, Guwahati 781 039, Assam, India

Received 2 September 2005
Available online 30 June 2006

Abstract

The conjugate heat transfer characteristics are studied for backward-facing step flow problem. Alternating direction implicit (ADI) method is used to find the steady state results for hydrodynamic solution using stream function–vorticity formulation. The energy equation in the fluid region and in the solid region are solved simultaneously. The conjugate effects are studied in connection with four parameters viz. *Re*, *Pr*, *k* and *b*. Effect of four parameters on local Nusselt number, interface temperature and average Nusselt number are presented in detail. The results are compared with non-conjugate case.

Keywords: Conjugate heat transfer; Backward step flow; Interface temperature; Nusselt number

1. Introduction

Fluid flow over a step occurs in many engineering applications. Backward-facing step (BFS) geometry is one of the most important benchmark problems used in computational fluid dynamics (CFD) to validate either a new algorithm or a computer code developed. It has an outflow boundary condition, flow separation, reattachment and several recirculation zones. Heat transfer characteristics in flow separation is important in engineering design aspect which leads to finding the local Nusselt number distribution and downstream temperature distribution. Conjugate heat transfer occurs when heat transfer in fluid region is coupled with heat transfer in solid region. The temperature and the heat fluxes at the solid–fluid interface are considered to be equal. The flow properties affect the heat transfer in solid region. Here the governing energy equations of solid and fluid regions have to be solved simultaneously. This is referred to as the fourth-kind boundary condition [1].

Recently conjugate heat transfer study is getting more attention by the researchers. Many publications are devoted to conjugate heat transfer on flat plate [2–5]. Vynnycky et al. [6] presented closed form relations for interface temperature, local Nusselt number and average Nusselt number for laminar flow over a flat plate as conjugate case. Chiu et al. [7] studied conjugate heat transfer of horizontal channel both experimentally and numerically. They found that the parametric study of operational parameters related to the conjugate heat transfer revealed that the addition of conjugate heat transfer significantly affects the temperature and heat transfer rates at the surface of the heated region. Rao et al. [8] presented the results for laminar mixed convection with surface radiation from a vertical plate with a heat source as conjugate case. They solved the governing equations by stream function–vorticity formulation. Jilani et al. [9] presented finite difference solution for conjugate heat transfer study on heat generating vertical cylinder. Steady [10] and unsteady [11] conjugate heat transfer from a cylinder in laminar flow are presented by Juncu. He carried out the numerical investigation for Reynolds number ranging from 2 to 20. He followed alternating direction implicit (ADI) method for solving the governing equations.

Recently Kanna and Das [12] presented closed form solution for laminar wall jet flow as conjugate case. They have reported closed form solution for local Nusselt

* Corresponding author. Tel.: +91 361 2690976; fax: +91 361 2690762.
E-mail address: manab@iitg.ernet.in (Manab Kumar Das).

0017-9310/$ - see front matter © 2006 Elsevier Ltd. All rights reserved.
doi:10.1016/j.ijheatmasstransfer.2006.02.058

Nomenclature

b	thickness of the slab
h	step height
H	channel height
i	x-direction grid point
j	y-direction grid point
k_f	thermal conductivity of the fluid, W/m K
k_s	thermal conductivity of the slab, W/m K
k	thermal conductivity ratio, k_s/k_f
Nu	local Nusselt number
$\overline{Nu}$	average Nusselt number
Pr	Prandtl number, $\frac{\nu}{\alpha}$
Re	Reynolds number for the fluid
T_w	constant bottom wall temperature
T_∞	constant inlet temperature
t	non-dimensional time
u, v	non-dimensional velocity components along (x, y) axes
x, y	non-dimensional Cartesian co-ordinates along and normal to the plate

Greek symbols

ε	convergence criterion
θ	dimensionless temperature
ψ	dimensionless stream function
ω	dimensionless vorticity

Subscripts

f	fluid
s	solid
w	wall
∞	inlet condition

number, interface temperature and average Nusselt number and validated the same by numerical simulations. Kanna and Das [13] have studied the conjugate heat transfer for two-dimensional (2D) laminar offset jet. They found that when Re is increased, the thermal boundary layer thickness is reduced. In solid slab, the effect of Re, Pr, slab thickness ratio, and k (ratio of thermal conductivities of solid and fluid) parameters are more significant near the recirculation region. When Re is increased, the slab temperature is reduced. Conjugate heat transfer study on laminar wall jet over backward-facing step is reported by Kanna and Das [14]. They found that the conjugate interface temperature value decreases along the step length and height. After expansion from the step its value is reduced to a minimum value followed by an increase. Local Nusselt number has peak value near the inlet due to entrainment and second peak occurs after reattachment of the jet.

The detailed hydrodynamic study on backward-facing step flow problem can be found in Armaly et al. [15], Gartling [16], Kim and Moin [17], Comini et al. [18], Barton [19] and many others. Bhattacharjee and Loth [20] have reported 2D DNS results for the BFS problem as a validation for their code to solve the wall jet flow problem. Recently Biswas et al. [21] have reported 2D as well as 3D BFS results. They reported the formation of Moffatt eddies as Re approaches zero.

The BFS problem is studied by Dyne and Heinrich [22], and also by Choudhury [23]. In addition to the fluid flow solution, they have solved the energy equation for the constant heat flux boundary condition. Dyne and Heinrich [22] have investigated the Nusselt (Nu) number distribution along the wall. It approaches fully developed value in the downstream direction. Mixed convective heat transfer in an inclined duct with backward-step geometry results are presented by Hong et al. [24]. The effects of inclination angle and the Prandtl number on the flow and heat transfer characteristics are reported. They found that the increase in inclination angle increases the reattachment length but decreases the wall friction coefficient. Kondoh et al. [25] studied the laminar heat transfer characteristics of backward-facing step flow problem. They studied the heat transfer characteristics in connection with expansion ratio, Reynolds number and Prandtl number. They reported local Nusselt number, peak Nusselt number and its location and thermal front. The effect of Prandtl is presented in detail. They found that the peak Nusselt number is not necessarily located at or very near to the reattachment location. Their reattachment length is slightly larger than the benchmark values of Armaly et al. [15].

It has been observed that several benchmark solutions are available in the literatures for closed as well as open domain. The conjugate heat transfer is an important area for research. However, there is no benchmark solutions available for conjugate heat transfer case. For BFS problem, the conjugate heat transfer study has not carried been carried out so far as a benchmark problem. The present investigation is aimed to find the conjugate heat transfer characteristics for backward-facing step flow problem in connection with Re, Pr, k and slab thickness.

2. Problem definition and numerical procedure

The geometry and boundary conditions for conjugate backward-facing step flow is shown in Fig. 1. The step height is assumed as half of the channel height ($h = H/2$). The hydrodynamic boundary conditions considered here are identical with those of Gartling [16] and Dyne and Heinrich [22]. The governing equations for incompressible

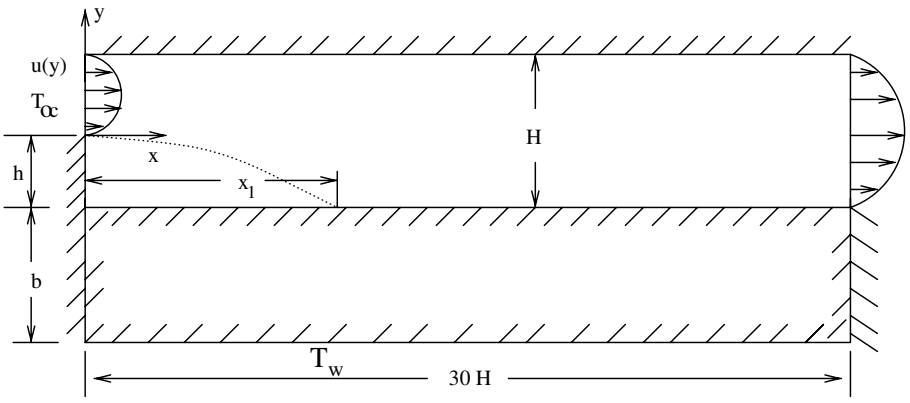

Fig. 1. Schematic diagram and boundary conditions in a conjugate BFS problem.

laminar flow are solved with a stream function–vorticity formulation. The transient form of the non-dimensional governing equations are

Stream function equation

$$\nabla^2\psi = -\omega \tag{1}$$

Vorticity equation

$$\frac{\partial\omega}{\partial t} + \frac{\partial(u\omega)}{\partial x} + \frac{\partial(v\omega)}{\partial y} = \frac{1}{Re}\nabla^2\omega \tag{2}$$

Energy equation

$$\frac{\partial\theta}{\partial t} + \frac{\partial(u\theta)}{\partial x} + \frac{\partial(v\theta)}{\partial y} = \frac{1}{RePr}\nabla^2\theta \tag{3}$$

Energy equation in solid region

$$\frac{\partial\theta_s}{\partial t} = \left(\frac{\alpha_s}{\alpha_f}\right)\frac{1}{RePr}\nabla^2\theta_s \tag{4}$$

where ψ – stream function, $u = \frac{\partial\psi}{\partial y}$; $v = -\frac{\partial\psi}{\partial x}$; $\omega = \frac{\partial v}{\partial x} - \frac{\partial u}{\partial y}$; θ – non-dimensional temperature, Pr = Prandtl number.

The solution approaches steady-state asymptotically. The computational domains considered here are clustered cartesian grids. The slab energy equation is written in transient non-dimensionalised form. The point to note here is that the second term (Eq. (4)) contains Re and Pr. It is arrived at in the following way. The dimensional form of energy equation in the solid region is $\frac{\partial T^*}{\partial t^*} = \alpha_s(\nabla^2 T^*)$. Since the time step is common to fluid region as well as solid region, time is non-dimensionalised by $t = \frac{t^*\overline{U}}{H}$ which leads to $\frac{\partial\theta}{\partial t} = \left(\frac{\alpha_s}{H\overline{U}}\right)(\nabla^2\theta)$ where $\overline{U}$ is the inlet mean velocity and $\frac{\alpha_s}{H\overline{U}} = \frac{\alpha_s}{\alpha_f}\cdot\frac{1}{RePr}$.

The non-dimensional form of the energy equation in the solid has been derived following Chiu et al. [7] and is also given in Kanna and Das [12,13]. The boundary conditions needed for the numerical simulation have been prescribed. The details of the discretization are given in Kanna and Das [26].

The boundary conditions needed for the numerical simulation have been prescribed (Fig. 1). Parabolic u velocity profile has been assumed at inlet ($u(y) = 12y - 24y^2$). The fluid at inlet has uniform temperature. At downstream boundary, the condition of zero first-derivative has been applied for velocity and temperature. The bottom wall is maintained at uniform constant temperature whereas the top wall is maintained as adiabatic condition. The initial conditions considered are zero for all the variables at time $t = 0$.

The stream function and vorticity at inlet is evaluated based on inlet u velocity profile. They are $\psi = 6y^2 - 8y^3$, $\omega = 12 - 48y$. At exit, the streamwise velocity gradients are assumed to be zero [27]. Thom's vorticity condition has been used to obtain the wall vorticity as given below.

$$\omega_w = -\frac{2(\psi_{w+1} - \psi_w)}{\Delta n^2} \tag{5}$$

where n is the grid spacing in the normal direction. Angirasa [28] has used this relation for the computation of buoyant wall jet.

Interface boundary condition

The conjugate boundary is shown in Fig. 2. Clustered grids are used for the computational domain. The conjugate boundary conditions are

$$k_s\left(\frac{\partial\theta_s}{\partial y}\right)_{y=0} = k_f\left(\frac{\partial\theta_f}{\partial y}\right)_{y=0} \quad \text{and} \quad \theta_f = \theta_s$$
$$\text{at interface } y = -h,\ 0 < x \leqslant 30 \tag{6}$$

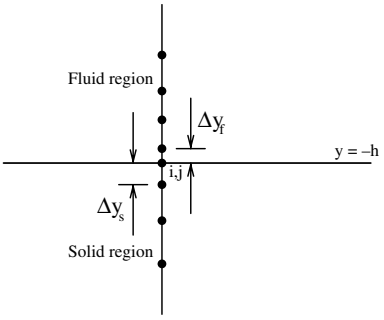

Fig. 2. Conjugate interface boundary grid points.

From Taylor series expansion the temperature gradients are evaluated and substituted in Eqs. (3), (4) and (6). Simplifying, the conjugate interface temperature at new time step is

$$\theta_{i,j}^{t+\Delta t} = \theta_{i,j}^{t} + \frac{2\Delta t}{RePr(\Delta y_f + k\Delta y_s)} \times \left(\frac{1}{2}(\Delta y_f + k\Delta y_s)\left(\frac{\theta_{f,i+1,j} - 2\theta_{f,i,j} + \theta_{f,i-1,j}}{\Delta x^2}\right) - k\frac{\theta_{s,i,j} - \theta_{s,i,j-1}}{\Delta y_s} + \frac{\theta_{f,i,j+1} - \theta_{f,i,j}}{\Delta y_f}\right)^t \quad (7)$$

The Nusselt number and average Nusselt number expressions are given by

$$Nu(x) = -\left.\frac{\partial\theta}{\partial y}\right|_{y=0} \quad (8)$$

$$\overline{Nu} = \frac{1}{L}\int_0^L Nu(x)\,dx \quad (9)$$

The parabolic equation (2) is solved by an alternate direction implicit (ADI) method [27]. The Poisson equation (1) is solved explicitly by a five point Gauss–Seidel method. With known velocity values Eq. (3) is solved by the ADI method. The energy equation in the fluid and solid regions are solved simultaneously. For the computation, time step 0.01 is used for $Pr = 0.71$, 10, 100.0, whereas for $Pr = 0.05$, 0.1, time step 0.001 is used. At steady state, the error reaches the asymptotic behavior. Here it is set as either the sum of temperature error from consecutive iteration reduced to either the convergence criteria ε (Eq. (10)) or a large total time is elapsed.

$$\sum_{i,j=1,1}^{i_{max},j_{max}} ((\theta_{s\,i,j}^{t+\Delta t} - \theta_{s\,i,j}^{t}) + (\theta_{f\,i,j}^{t+\Delta t} - \theta_{f\,i,j}^{t})) < \varepsilon \quad (10)$$

3. Validation of the code

The hydrodynamic solution obtained for backward-facing step flow problem has been compared with benchmark results. The primary vortex reattachment length is compared with Armaly et al. [15], Kim and Moin [17] and Gartling [16]. The downstream location u and v velocities are compared with Gartling [16] and found good agreement between them. This detailed results can be found in Kanna and Das [29]. Heat transfer solution is obtained for non-conjugate case. The top and bottom walls are assumed at constant heat flux condition. The downstream temperature results are compared with Dyne and Heinrich [22] (Fig. 3) and excellent agreement has been obtained. Kondoh et al. [25] have presented heat transfer results for different expansion ratios. They reported that the reattachment length is slightly larger than the benchmark results. For expansion ratio (ER) = 2 and $Re = 100$ case, the reattachment length is $x_1 \simeq 4.8h$ whereas the benchmark value is $x_1 \simeq 2.7h$ [19,20,29]. Since this discrepancy will be reflected on the heat transfer characteristics, in the present validation no attempt has been given to compare with the results of Kondoh et al. [25].

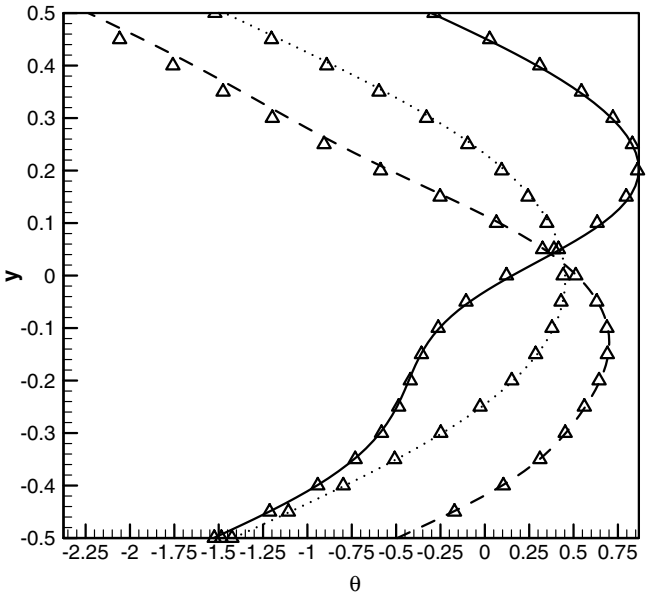

Fig. 3. Comparison of numerical solution with benchmark results. (△) Dyne and Heinrich [22] and present: (—) $x = 3$, (---) $x = 7$, (···) $x = 15$.

4. Grid independence study

For the BFS problem, grids are clustered near the high gradients zone (Fig. 4). Since grids in both the directions are clustered, a systematic grid independence study is carried out by Kanna and Das [29] for the y-direction as well as in the x-direction. In the y-direction different grid systems are tested and variation in reattachment length is less than 1%. A similar study is carried out for x-direction with 101×81, 131×81, 151×81 and 201×81 grid points and it is concluded that 151×81 grid points could be used for all the calculations for finding hydrodynamic solution [29]. For solid region the grids are chosen based on average Nusselt number variation less than 1% in the normal direction for $b \leqslant 5h$ and 41 grid points are to be used for $b > 5h$ cases. In the solid region, uniform grid points are used in the normal direction whereas in the streamwise direction 151 grids are clustered similar to the fluid region. This system of clustering grids are identical with Kanna and Das [13].

5. Results and discussion

Conjugate heat transfer study is carried out in backward-facing step flow problem considering four parameters viz. Re, Pr, k and b. Effect of these parameters on local Nusselt number, conjugate interface temperature and average Nusselt number are presented in detail. Isotherm patterns are shown for the case considered here. Peak Nusselt number and its location for different Reynolds number is listed. Downstream location temperature are tabulated for comparison. To demonstrate the effect of

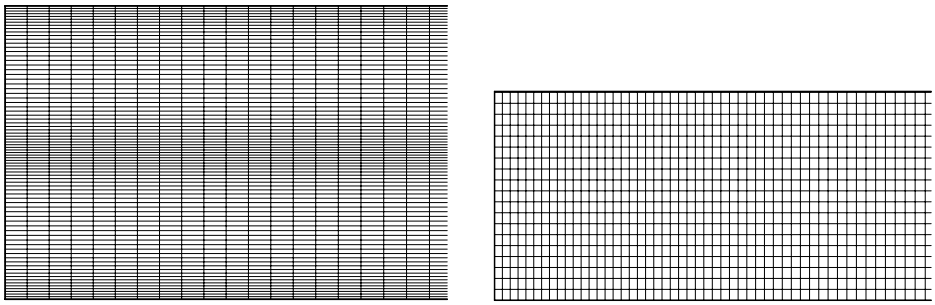

(a) Fluid region clustered grids (b) Solid region grids

Fig. 4. A part of the grids used for the computation.

conjugate condition, non-conjugate study is carried out with $b = 0$ and $\theta = 1$ at $y = -h$. The variables considered for the study are as follows. The Reynolds number range is from 100 to 800 and the Prandtl number range is from 0.05 to 100. In many practical situations, the conductivity of solid is greater than the fluid conductivity. Here the conductivity ratios are considered greater than 1 and maximum of 20. Slab thickness range considered is from $1h$ to $20h$.

Isotherm for different cases are shown in Fig. 5–12. Results are shown up to channel length equals to $x = 20h$. Fig. 5 shows the effect of *Re* on the isotherm in the fluid region for conjugate and non-conjugate cases. The conjugate study is presented for $Pr = 0.71$, $k = 10$, $b = 4h$ and non-conjugate results are presented for $Re = 800$, $Pr = 0.71$. In the fluid region the isotherms are clustered near the reattachment location (Fig. 5(a)) and further downstream location it is spreading in the normal direction. When *Re* increases this deflection of temperature contour is shifted (Fig. 5(b) and (c)) in the downstream direction. This is mainly due to the shift in the reattachment location in the downstream direction at higher *Re*. It is noticed that the spread of temperature in the normal direction is reduced due to the formation of upper wall vortex at higher *Re*. The temperature for non-conjugate case (Fig. 5(d)) is higher compared to those for conjugate results (Fig. 5(c)) for the same *Re* and *Pr*. The flow property *Re* affects the heat transfer in the solid region (Fig. 6). The two-dimensionality is well captured in the solid region. It is noticed that in the normal direction the non-dimensional temperature is decreased due to the cooling effect along the interface at $y = -h$ (Fig. 6(a)). It is observed that near the bottom wall, temperature contours are showing linear trend (Fig. 6(a)–(c)). Near the reattachment location, a non-linear trend is observed. This non-linearity in the isotherm is moving downstream when *Re* is increased

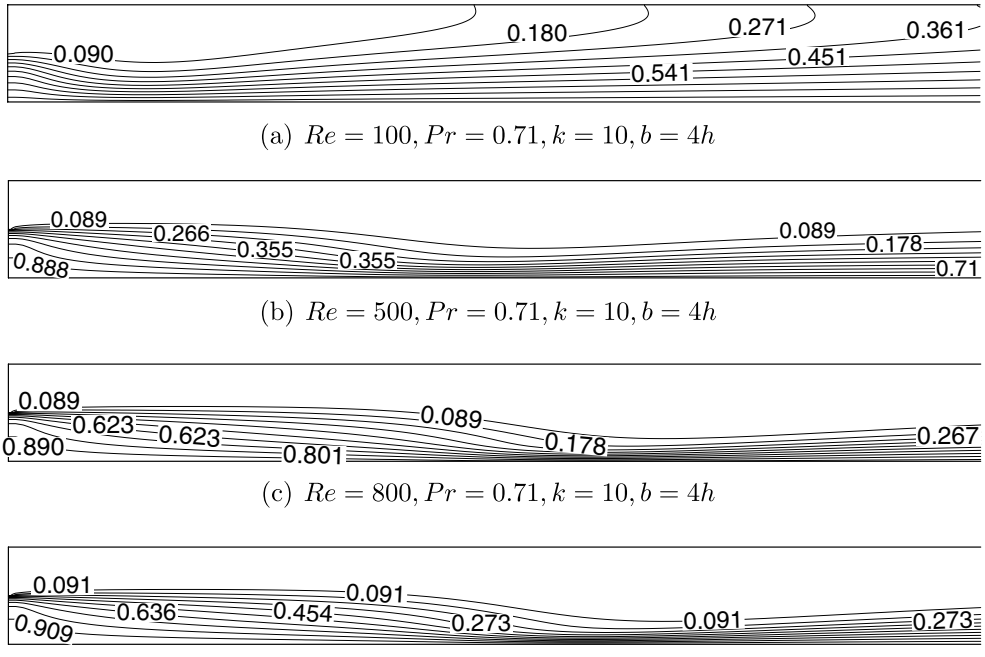

(a) $Re = 100, Pr = 0.71, k = 10, b = 4h$

(b) $Re = 500, Pr = 0.71, k = 10, b = 4h$

(c) $Re = 800, Pr = 0.71, k = 10, b = 4h$

(d) Non-conjugate case: $Re = 800, Pr = 0.71$

Fig. 5. Effect of *Re* on isotherm in the fluid region.

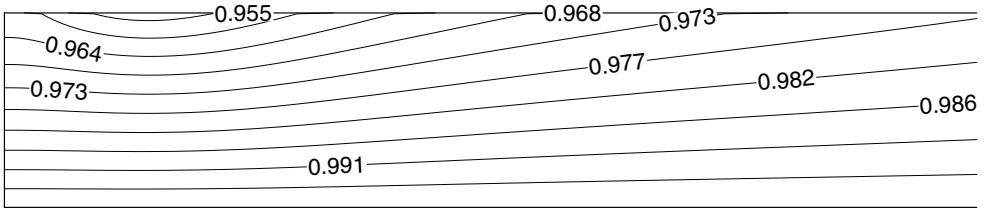

(a) $Re = 100$

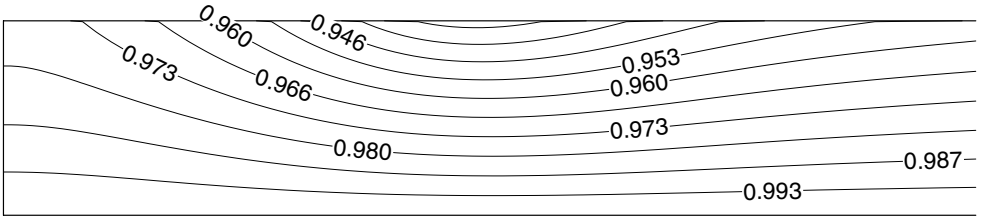

(b) $Re = 500$

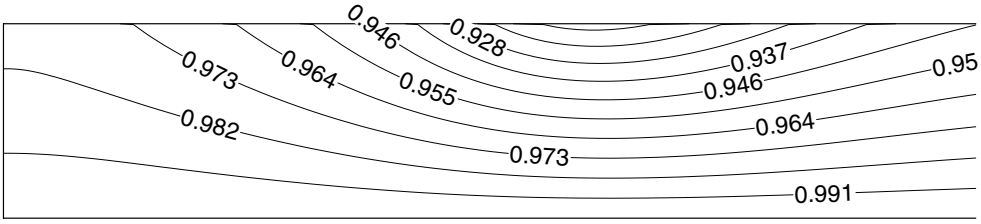

(c) $Re = 800$

Fig. 6. Effect of *Re* on isotherm in the solid region ($Pr = 0.71$, $k = 10$, $b = 4h$).

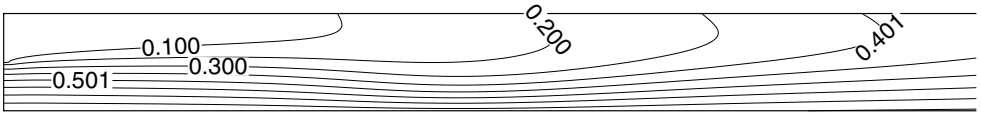

(a) $Pr = 0.1$

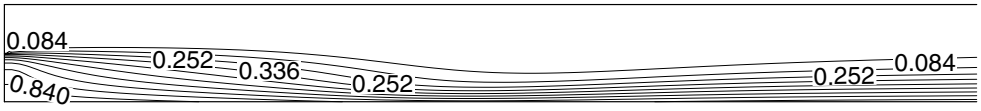

(b) $Pr = 0.71$

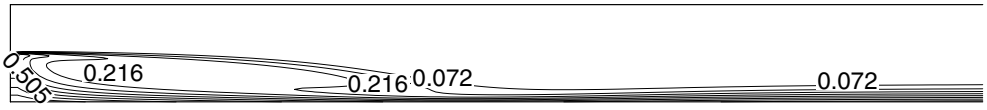

(c) $Pr = 10$

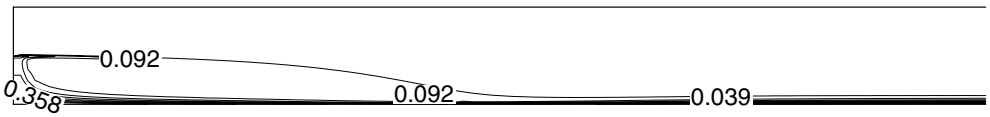

(d) $Pr = 100$

Fig. 7. Effect of *Pr* on isotherm in the fluid region ($Re = 500$, $k = 2$, $b = 2h$).

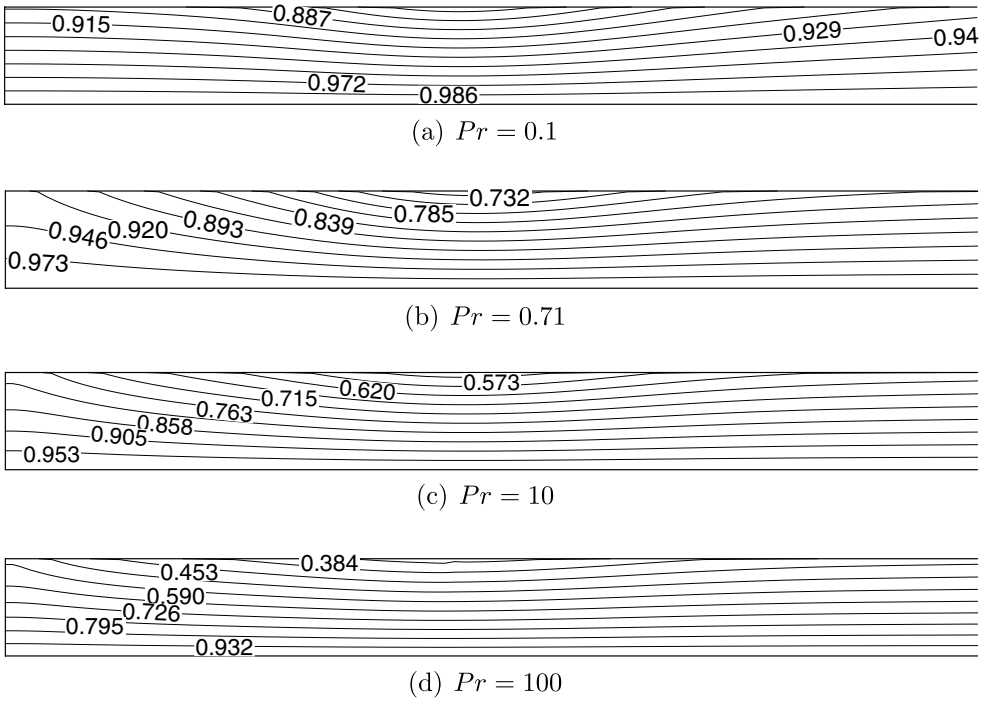

Fig. 8. Effect of Pr on isotherm in the solid region ($Re = 500$, $k = 2$, $b = 2h$).

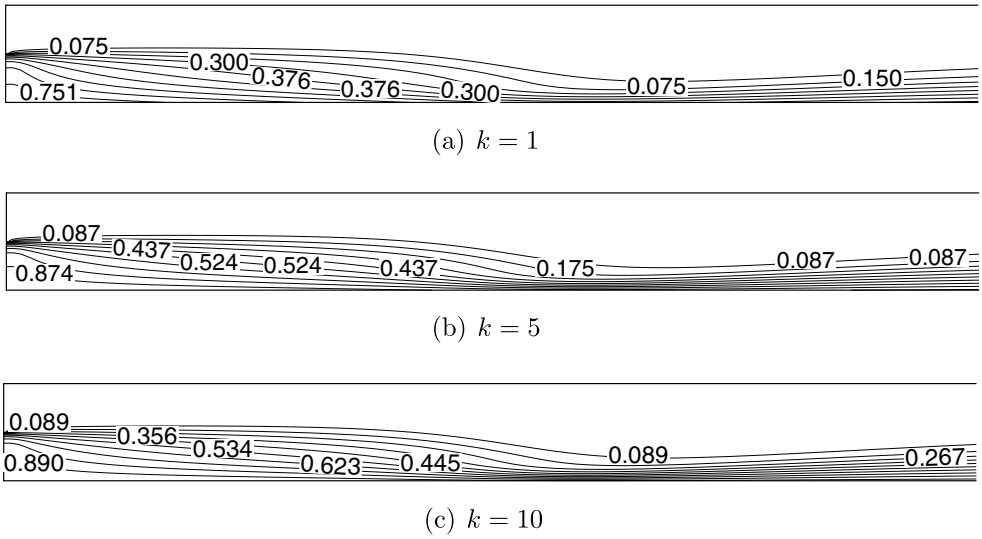

Fig. 9. Effect of k on isotherm in the fluid region ($Re = 800$, $Pr = 0.71$, $b = 4h$).

(Fig. 6(c)). It is noticed that near the reattachment location temperature attains a lower value than the other parts of the solid slab.

Influence of Prandtl number on conjugate heat transfer is shown in Figs. 7 and 8. Effect of Prandtl number ($Pr = 0.1$, 0.71, 10 and 100) is presented for $Re = 500$, $k = 2$, $b = 2h$. At $Pr = 0.1$ isotherm is well spread in the domain (Fig. 7(a)). It is noticed that the fluid attains a higher temperature in the downstream direction. When Pr is increased, the temperature contours are clustered near the bottom wall (Fig. 7(b)–(d)) and the thermal boundary layer thickness is reduced i.e. convection mode of heat transfer is dominant (Fig. 7(d)). At higher Pr, the influence of inlet fluid is dominant in the fluid region heat transfer. However in the recirculation region thermal boundary layer thickness is not much affected by the changes in Pr. Influence of fluid property Pr on solid slab is shown in Fig. 8. At $Pr = 0.1$, the heat transfer in the slab mostly controlled by conduction. However near the reattachment location, a non-linearity is observed (Fig. 8(a)). When Pr increases, the temperature in the solid is decreased in the domain (Fig. 8(b)–(d)).

Effect of solid to fluid thermal conductivity ratio (k) on isotherm is shown in Figs. 9 and 10. It is noticed that the

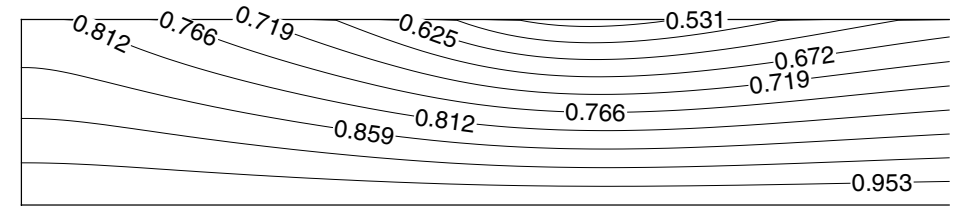

(a) $k = 1$

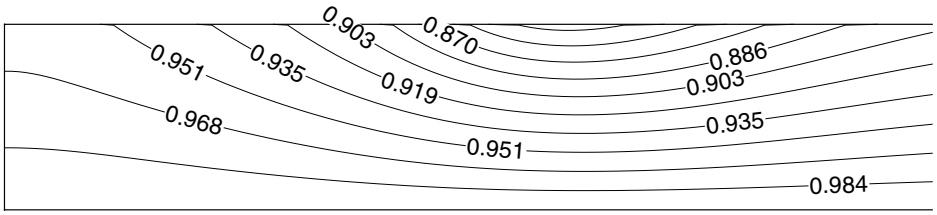

(b) $k = 5$

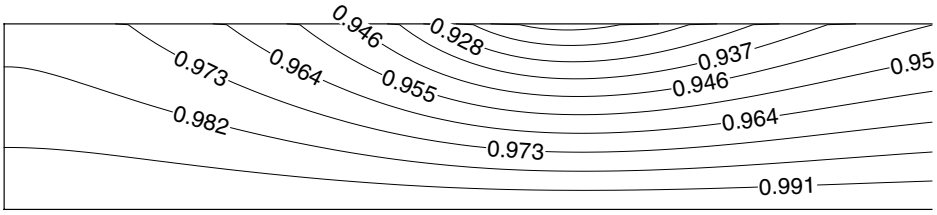

(c) $k = 10$

Fig. 10. Effect of k on isotherm in the solid region ($Re = 800$, $Pr = 0.71$, $b = 4h$).

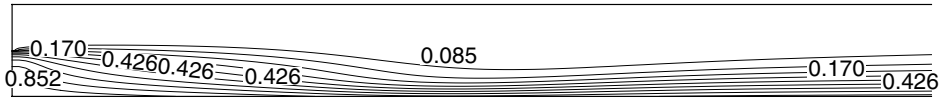

(a) $b = 1$h

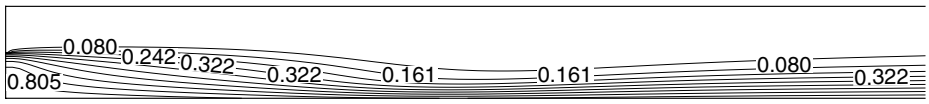

(b) $b = 5$h

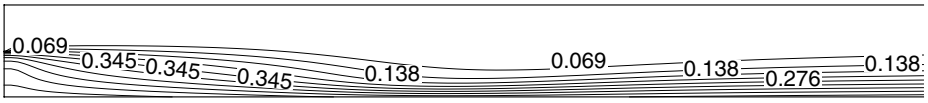

(c) $b = 10$h

Fig. 11. Effect of b on isotherm in the fluid region ($Re = 500$, $Pr = 0.71$, $k = 2$).

increment in k is reflected on the temperature value (Fig. 9(a)–(c)). When k increases, temperature is increased. It is observed that there is less variation in thermal layer thickness with increase in k. The significance of k variations on the solid temperature are presented in Fig. 10. When k is increased, the temperature in solid slab is increased. A non-linear trend in the temperature contour is noticed. This trend is similar for different k values considered here for the study. Effect of solid slab thickness is presented in Figs. 11 and 12 where temperature in fluid region and solid region in connection with b are presented. Results are presented for $b = 1$, 5 and 10. Increment in bottom wall thickness has an effect on the temperature contour in the fluid region. The magnitude of the temperature is reduced when b is increased (Fig. 11(a)–(c)). However the thermal layer size is less

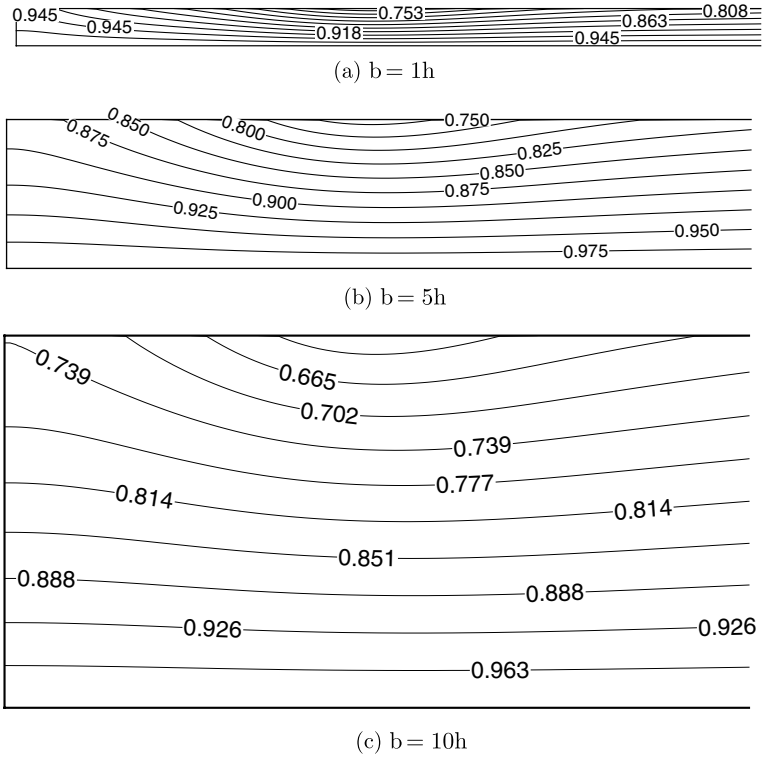

Fig. 12. Effect of b on isotherm in the solid region ($Re = 500$, $Pr = 0.71$, $k = 2$).

affected by variations in b. Temperature contour in solid slab is shown for different b values. The minimum temperature values is occurred near the reattachment location (Fig. 12(a)). Near this location, a non-linear trend is observed in the solid region. When b is increased, the temperature in normal direction is reduced (Fig. 12(b) and (c)) because the thermal resistance is more.

The conjugate interface temperature is found from the computations and presented for the four parameters (Fig. 13). Effect of Re on the interface temperature is shown in Fig. 13(a). The interface temperature is decreased near to the reattachment point and increases again in the downstream direction. When Re is increased, interface temperature is decreased (Fig. 13(a)). This means that, according to Newton's law of cooling, the convective heat transfer is increased. The effect of Pr on interface temperature is shown in Fig. 13(b). It is noticed that the interface temperature is decreased to a minimum value and further is increased in the downstream direction. When Pr is increased the interface temperature is decreased. It is found that the location for minimum interface value ($x = 9.41h$) is not changed with Pr. Fig. 13(c) shows the effect of k on interface temperature. The interface temperature is reduced to a minimum value and further it is increased. It is noticed that at $k \geqslant 5$ in downstream direction it approaches fully developed condition. When k is increased the interface is approaching the bottom wall temperature i.e. it behaves like a non-conjugate case. Effect of b are shown in Fig. 13(d) and (e). The interface temperature is reduced to a minimum value and further it is increased. When b is increased the interface temperature value is reduced. When b is increased, it is noticed that up to $b \leqslant 5$, near the reattachment location the minimum interface temperature value is increased (Fig. 13(d)). This behavior is verified with different values of Re and k (Fig. 13(e)). At three downstream locations $x = 6h$, $14h$, $30h$, temperature values are listed in Table 1 and the same is presented in Fig. 14. These locations cover upstream of reattachment location and immediate downstream and far downstream to reattachment point. Due to the formation of upper wall vortex at $x = 14h$, the thermal layer thickness is smaller than other two locations.

Local Nusselt number distribution is shown in Fig. 15. Fig. 15(a) shows the effect of Re on Nu. Nusselt number is increased to a peak value and further is decreased in downstream direction. Increment in Re increases convection heat transfer, and thus Nu is increased for higher value of Re. Effect of Pr on Nu is shown in Fig. 15(b). Nusselt number is increasing to a maximum value and further is decreased. At $Pr = 0.1$ conduction mode of heat transfer is predominant thus Nu is having smaller value. When Pr is increased local Nusselt number value is increased. It is noticed at $Pr = 100$ a kink is observed near the reattachment location. Fig. 15(c) shows the effect of k on Nu. Nu is increased to a peak value and further it is decreased in the downstream direction. Nu is having small variation upto $x \simeq 3.83h$. It is noticed that when k is increased Nu is increased. It is observed that $k \geqslant 5$ has less significance

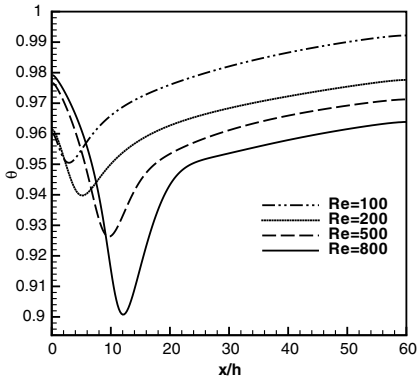

(a) Effect of Re:(Pr = 0.71, k = 10, b = 4h)

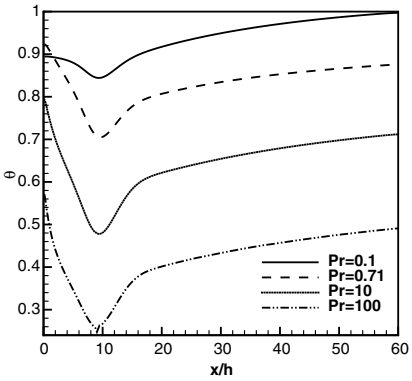

(b) Effect of Pr:(Re = 500, k = 2, b = 2h)

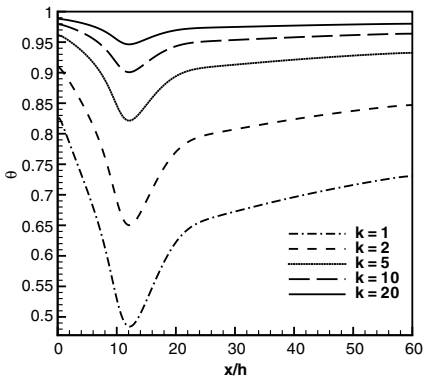

(c) Effect of k:(Re = 800, Pr = 0.71, b = 4h)

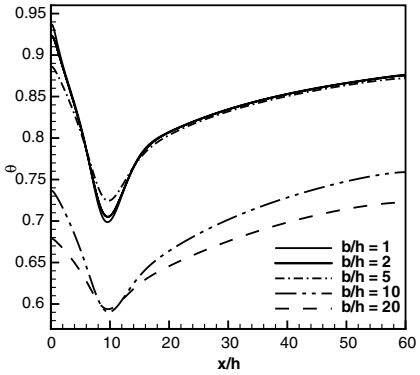

(d) Effect of b:(Re = 500, Pr = 0.71, k = 2)

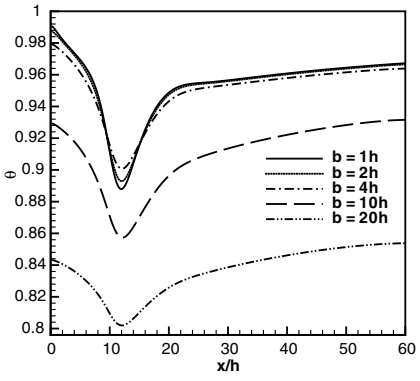

(e) Effect of b:(Re = 800, Pr = 0.71, k = 10)

Fig. 13. Effect of *Re*, *Pr*, *k* and *b* on the interface temperature.

Table 1
Downstream location temperature in the fluid region

y	$x = 6h$	$x = 14h$	$x = 30h$
−0.500	0.978	0.906	0.953
−0.445	0.849	0.625	0.827
−0.395	0.754	0.377	0.702
−0.344	0.667	0.206	0.582
−0.294	0.592	0.117	0.470
−0.243	0.527	0.071	0.368
−0.192	0.467	0.042	0.281
−0.142	0.405	0.023	0.208
−0.091	0.331	0.012	0.149
−0.041	0.246	0.006	0.105
0.010	0.156	0.003	0.072
0.060	0.080	0.001	0.050
0.111	0.032	0.001	0.034
0.162	0.009	0.001	0.024
0.212	0.002	0.001	0.017
0.263	0.000	0.001	0.013
0.313	0.000	0.001	0.011
0.364	0.000	0.001	0.009
0.465	0.000	0.001	0.009
0.500	0.000	0.000	0.008

$Re = 800$, $Pr = 0.71$, $k = 10$, $b = 4h$.

on *Nu* beyond the reattachment location. Fig. 15(d) shows the effect of slab thickness on local Nusselt number distribution. It is noticed that *Nu* is increased to a maximum value and further it is decreased in the downstream direction. When *b* is increased upto 4*h* the variation in *Nu* is small. Peak *Nu* in this range is, $Nu = 6.53(b = 1h)$, $=6.58(b = 2h)$, $=6.66(b = 4h)$. It is noticed that upto $b = 4h$ the peak *Nu* is increased and for higher *b* values it is decreased (peak $Nu = 6.34(b = 10h)$, $=5.96(b = 20h)$).

Average Nusselt number is calculated for the cases considered in the present study. Table 2 shows the effect of *Re* on $\overline{Nu}$. It is noticed that the $\overline{Nu}$ is increased when *Re* is increased. It is found that the percent increment in $\overline{Nu}$ is reduced and may reach an asymptotic value (Fig. 16). $\overline{Nu}$ for different *Pr* is listed in Table 3 for $Re = 500$, $k = 2$, $b = 2h$. When *Pr* is increased $\overline{Nu}$ is increased. Effect of thermal conductivity ratio on $\overline{Nu}$ is shown in Table 4. Average *Nu* for non-conjugate case is presented for comparison. It is noticed that when *k* is increased $\overline{Nu}$ is increased. It is observed that when *k* is increased $\overline{Nu}$ approaches the non-conjugate value. Effect of *b* on $\overline{Nu}$ is presented in Tables 5 and 6. When *b* is increased $\overline{Nu}$ is decreased. It is noticed that the decrement in $\overline{Nu}$ is more significant at $b \geqslant 5$. Peak Nusselt number and its location for $Pr = 0.71$, $k = 10$, $b = 4h$ and different *Re* is listed in Table 7. When *Re* is increased the peak $\overline{Nu}$ is increased. It is noticed that the location (x/h) of peak $\overline{Nu}$ is always downstream of the reattachment location (x_1/h).

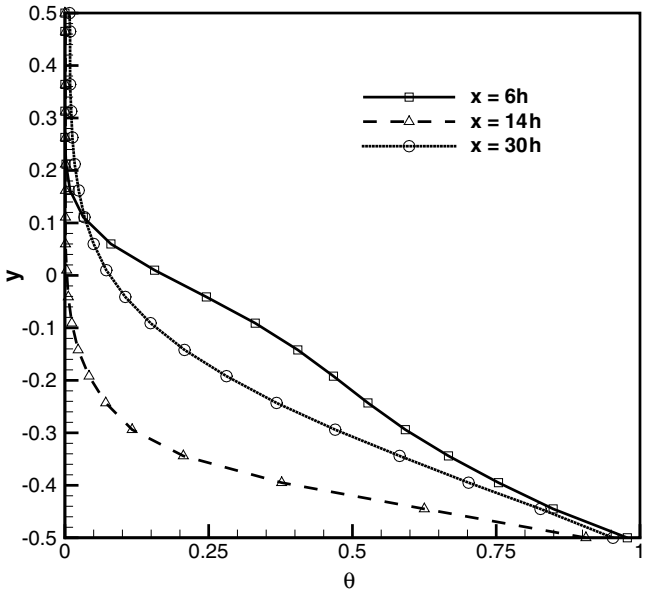

Fig. 14. Downstream location temperature in the fluid region ($Re = 800$, $Pr = 0.71$, $k = 10$, $b = 4h$).

Table 2
Effect of *Re*

Re	$\overline{Nu}$	Percentage of increase in $\overline{Nu}$
100	0.97	–
200	1.49	53.61
300	1.79	20.13
400	1.99	11.17
500	2.16	8.54
600	2.32	7.41
700	2.45	5.60
800	2.56	4.49
800	2.68 (non-conjugate)	–

$Pr = 0.71$, $k = 10$, $b = 4h$.

6. Conclusions

The conjugate heat transfer study of the backward-facing step benchmark problem is solved as the asymptotic solution of the time dependent stream function–vorticity formulation. The discretization has been done by ADI method with centered space. The study is carried out with four parameters viz. *Re*, *Pr*, *k* and *b*. Effect of these parameters

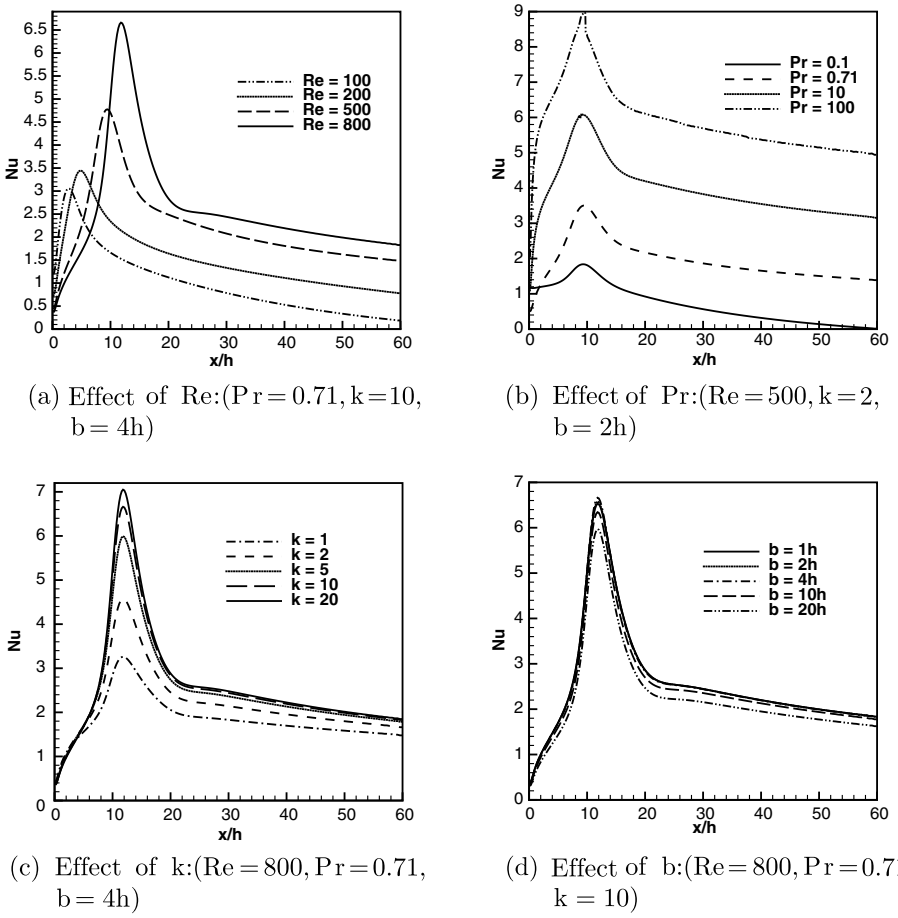

(a) Effect of Re:(Pr = 0.71, k = 10, b = 4h)

(b) Effect of Pr:(Re = 500, k = 2, b = 2h)

(c) Effect of k:(Re = 800, Pr = 0.71, b = 4h)

(d) Effect of b:(Re = 800, Pr = 0.71, k = 10)

Fig. 15. Effect of *Re*, *Pr*, *k* and *b* on the local Nusselt number.

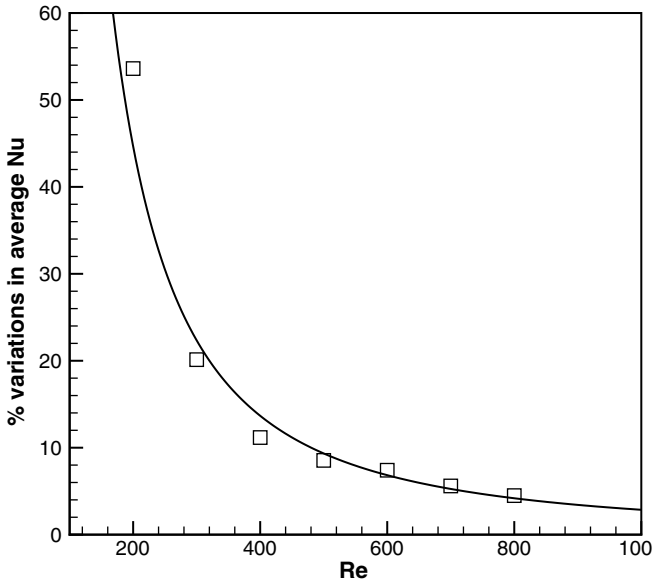

Fig. 16. Percentage of variations in average Nusselt number ($Pr = 0.71$, $k = 10$, $b = 4h$).

Table 3
Effect of Pr

Pr	$\overline{Nu}$
0.05	0.254
0.1	0.684
0.71	1.893
10	3.867
100	5.789

$Re = 500$, $k = 2$, $b = 2h$.

Table 4
Effect of k

k	$\overline{Nu}$	% difference with non-conjugate case
1	1.82	32.08
2	2.17	19.02
5	2.44	8.95
10	2.56	4.48
20	2.61	2.61
Non-conjugate	2.68	–

$Re = 800$, $Pr = 0.71$, $b = 4h$.

Table 5
Effect of b

b/h	$\overline{Nu}$
1	1.894
2	1.893
5	1.887
10	1.607
20	1.543

$Re = 500$, $Pr = 0.71$, $k = 2$.

on local Nusselt number, interface temperature and average Nusselt number is reported in details. The following conclusions are drawn.

The temperature contours are deflected towards the bottom wall in fluid region at higher Re. Flow property Re has a significant effect on the isotherm in the solid region. High thermal gradients are observed near the reattachment location in the solid region. Thermal layer thickness is reduced when Pr is increased in the downstream of the reattachment location. In solid region the magnitude of the temperature is reduced for higher Pr. Increment in k increases temperature in the fluid as well as in the solid region. This effect is reverse for b. The interface temperature is reduced to a minimum value and further it is increased in the downstream direction. When k is increased the interface temperature approaches the bottom wall temperature. Local Nusselt number is increased to a maximum value and further it is decreased in the downstream direction. When Re is increased peak Nu is increased. The peak Nu occurs downstream to the reattachment location. When k is increased Nu is increased. The peak Nu location is occurred at the same location for the k values considered. When b is increased the peak Nu is increased upto $b \leqslant 5$ and for $b > 5$ it is decreased. The average Nusselt number is increased for higher Re. This increment is reduced as Re is gradually increased and may approach an asymptotic value. $\overline{Nu}$ is increased when Pr is increased. The effect of k on $\overline{Nu}$ is studied and compared with non-conjugate case. When k is increased $\overline{Nu}$ is increased. It is found that the solution approaches non-conjugate value when $k \geqslant 20$ for $Re = 800$, $Pr = 0.71$, $b = 4h$. When b is increased $\overline{Nu}$ is reduced. Variation in $\overline{Nu}$ is small when $b \leqslant 5$.

Table 6
Effect of b

b/h	$\overline{Nu}$
1	2.559
2	2.557
4	2.550
10	2.448
20	2.249

$Re = 800$, $Pr = 0.71$, $k = 4$.

Table 7
Peak Nusselt number and its location

Re	$\overline{Nu}$	x/h	x_1/h
100	3.05	2.71	2.55
200	3.44	4.85	4.71
500	4.78	9.43	9.41
800	6.66	11.82	11.58

$Pr = 0.71$, $k = 10$, $b = 4h$.

References

[1] A.V. Luikov, V.A. Aleksashenko, A.A. Aleksashenko, Analytical methods of solution of conjugated problems in convective heat transfer, Int. J. Heat Mass Transfer 14 (1971) 1047–1056.
[2] A.V. Luikov, Conjugate convective heat transfer problems, Int. J. Heat Mass Transfer 17 (1974) 257–265.
[3] P. Payvar, Convective heat transfers to laminar flow over a plate of finite thickness, Int. J. Heat Mass Transfer 20 (1971) 431–433.
[4] I. Pop, D.B. Ingham, A note on conjugate forced convection boundary layer flow past a flat plate, Int. J. Heat Mass Transfer 36 (1993) 3873–3876.

[5] A. Pozzi, M. Lupo, The coupling of conduction with forced convection over a flat plate, Int. J. Heat Mass Transfer 32 (1989) 1207–1214.
[6] M. Vynnycky, S. Kimura, K. Kanev, I. Pop, Forced convection heat transfer from a flat plate: the conjugate problem, Int. J. Heat Mass Transfer 41 (1998) 45–59.
[7] W.K.S. Chiu, C.J. Richards, Y. Jaluria, Experimental and numerical study of conjugate heat transfer in a horizontal channel heated from below, J. Heat Transfer 123 (August) (2001) 688–697.
[8] C.G. Rao, C. Balaji, S.P. Venkateshan, Conjugate mixed convection with surface radiation from a vertical plate with a discrete heat source, J. Heat Transfer 123 (August) (2001) 698–702.
[9] G. Jilani, S. Jayaraj, M.A. Ahmad, Conjugate forced convection–conduction heat transfer analysis of a heat generating vertical cylinder, Int. J. Heat Mass Transfer 45 (2002) 331–341.
[10] Gh. Juncu, Conjugate heat/mass transfer from a circular cylinder with an internal heat/mass source in laminar crossflow at low Reynolds numbers, Int. J. Heat Mass Transfer 48 (2005) 419–424.
[11] Gh. Juncu, Unsteady conjugate heat/mass transfer from a circular cylinder in laminar crossflow at low Reynolds numbers, Int. J. Heat Mass Transfer 47 (2004) 2469–2480.
[12] P.R. Kanna, M.K. Das, Conjugate forced convection heat transfer from a flat plate by laminar plane wall jet flow, Int. J. Heat Mass Transfer 48 (2005) 2896–2910.
[13] P.R. Kanna, M.K. Das, Conjugate heat transfer study of two-dimensional laminar incompressible offset jet flows, Numer. Heat Transfer A 48 (2005) 671–691.
[14] P.R. Kanna, M.K. Das, Conjugate heat transfer study of two-dimensional laminar incompressible wall jet over backward-facing step, J. Heat Transfer, submitted for publication.
[15] B.F. Armaly, F. Durst, J.C.F. Pereira, B. Schonung, Experimental and theoretical investigation of backward-facing step flow, J. Fluid Mech. 127 (1983) 473–496.
[16] D.K. Gartling, A test problem for outflow boundary conditions-flow over a backward-facing step, Int. Numer. Meth. Fluids 11 (1990) 953–967.
[17] J. Kim, P. Moin, Application of a fractional-step method to incompressible Navier–Stokes equations, J. Comput. Phys. 59 (1985) 308–323.
[18] G. Comini, M. Manzan, C. Nonino, Finite element solution of the streamfunction-voriticity equations for incompressible two-dimensional flows, Int. J. Numer. Meth. Fluids 19 (1994) 513–525.
[19] I.E. Barton, The entrance effect of laminar flow over a backward-facing step geometry. International, J. Numer. Meth. Fluids 25 (1997) 633–644.
[20] P. Bhattacharjee, E. Loth, Simulations of laminar and transitional cold wall jets, Int. J. Heat Fluid Flow 25 (2004) 32–43.
[21] G. Biswas, M. Breuer, F. Durst, Backward-facing step flows for various expansion ratios at low and moderate Reynolds numbers, J. Fluids Eng. 126 (May) (2004) 362–374.
[22] B.R. Dyne, J.C. Heinrich, Flow over a backward-facing step: a bench mark problem for laminar flow with heat transfer. Benchmark problems for heat transfer codes, HTD-V 222 (1992) 73–76.
[23] D. Choudhury, A numerical study of laminar flow and heat transfer in a backward-facing step using fluent: a finite-volume CFD. Benchmark problems for heat transfer codes, ASME, HTD-v 222 (1992) 53–56.
[24] B. Hong, B.F. Armaly, T.S. Chen, Laminar mixed convection in a duct with a backward-facing step: the effects of inclination angle and Prandtl number, Int. J. Heat Mass Transfer 12 (1993) 3059–3067.
[25] T. Kondoh, Y. Nagano, T. Tsuji, Computational study of laminar heat transfer downstream of a backward-facing step, Int. J. Heat Mass Transfer 36 (3) (1993) 577–591.
[26] P.R. Kanna, M.K. Das, Numerical simulation of two-dimensional laminar incompressible offset jet flows, Int. J. Numer. Meth. Fluids 49 (4) (2005) 439–464.
[27] P.J. Roache, Fundamentals of Computational Fluid Dynamics, Hermosa, USA, 1998 (Chapter 3).
[28] D. Angirasa, Interaction of low-velocity plane jets with buoyant convection adjacent to heated vertical surfaces, Numer. Heat Transfer A 35 (1999) 67–84.
[29] P.R. Kanna, M.K. Das, A short note on the reattachment length for BFS problem, Int. J. Numer. Meth. Fluids 50 (6) (2006) 683–692.